ELSEVIER

Thermochimica Acta 282/283 (1996) 165–173

thermochimica acta

Diffusion and phase diagram in binary alloys[1]

J. Mimkes [a,*], M. Wuttig [b]

[a] *FB Physik, University GH Paderborn, 33095 Paderborn, Germany*
[b] *Department of Nuclear and Chemical Engineering, University of Maryland, College Park, MD 20740, USA*

Abstract

The relationship between diffusion and phase diagram is discussed in more detail for Ag–Au and Au–Ni alloys. For each alloy tracer diffusion and interdiffusion data have been compared with the corresponding phase diagram.

Tracer diffusion is related to the solid–liquid phase transition. Ag and Au tracer diffusivities $D^*(x)$ in Ag–Au alloys and melting temperature $T_m(x)$ of Ag–Au show opposite curvatures. The same holds for D^* of Au and Ni in Au–Ni alloys and indicates a vacancy diffusion mechanism.

Interdiffusion depends on the critical temperature of the solid–solid phase transition of the phase diagram. The curvature of interdiffusivity $D(x)$ is determined by the sign of $T_c(x)$ or the interaction energy ε of the regular alloy. The calculations agree well with the experimental data.

Keywords: Ag–Au alloy; Au–Ni alloy; Interdiffusion; Melting temperature; Phase diagram; Tracer diffusion; Vacancy diffusion

1. Introduction

Recent developments in thin film technology and multilayer structures have led to an increased interest in interdiffusion of alloys [1–3]. Thin films produced by molecular beam epitaxy as well as metal contacts may become unstable or deteriorate, owing to interdiffusion, if the films are exposed to high temperatures during manufacturing processes.

It is the object of this paper to discuss the close relationship between diffusion and phase diagrams and to compare tracer and interdiffusion data with the phase diagrams of the two binary alloys Ag–Au and Au–Ni, as these alloys mix in the complete range of composition.

* Corresponding author.

[1] Dedicated to Takeo Ozawa on the Occasion of his 65th Birthday.

SSDI 0040-6031(96)02815-8

2. Diffusion and interdiffusion

Diffusion in alloys is always an interdiffusion of all the atoms of the solid and depends on the tracer diffusivity of each component. The models of tracer diffusion and interdiffusion in binary alloys are well established in the literature [4–8]. At a concentration x of component B the coefficient $D(x)$ of interdiffusivity in a binary alloy is given by [8]

$$D(x) = \{xD^*_A(x) + (1-x)D^*_B(x)\}\gamma(x)$$

$$D(x) = D^*_{B\text{ in }A}(x) \quad x \ll 1$$

$$D(x) = D^*_{A\text{ in }B}(x) \quad x \cong 1 \tag{1}$$

Interdiffusion depends on the tracer diffusivities $D^*_A(x)$ and $D^*_B(x)$ of the components A and B, as well as on the thermodynamic factor $\gamma(x)$.

At small concentrations of component B, x will be close to $x = 0$ and the thermodynamic factor equals unity, $\gamma(x) = 1$. Interdiffusion will then be equivalent to impurity diffusion of tracer B in the nearly pure A metal. For very large concentrations, x will be close to $x = 1$, $\gamma(x)$ again equals one and interdiffusion is equal to impurity diffusion of tracer A in the nearly pure B metal. At all other concentrations, x, interdiffusion is equivalent to an effective impurity diffusion.

3. Tracer diffusion

Tracer diffusion is the diffusion of a single (radioactive) tracer in the matrix of an alloy and will depend on its composition. Fig. 1 shows tracer diffusion data of Au and

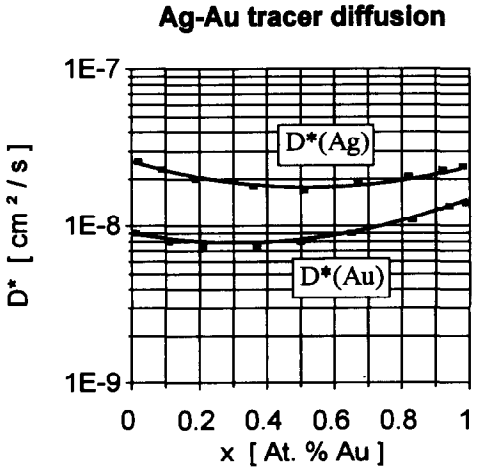

Fig. 1. Tracer diffusion of Ag and Au in Ag–Au alloys as a function of composition x. Data points from Ref. [9], solid line according to Eq. (7).

Ag in Au–Ag alloys [9] at 900°C, x is the concentration of component B (=Ag). The tracer diffusivity D_A^* of a tracer A (Au) is equivalent to selfdiffusion for $x=0$ (no B atoms) and equivalent to impurity diffusion of Au in Ag for $x \to 1$. Tracer diffusivity D_B^* of a tracer B (Ag) is equivalent to selfdiffusion for $x=1$ (no A atoms) and equivalent to impurity diffusion of Ag in Au for $x \to 0$.

D_A^* is determined by

$$D_A^*(x) = D_{A0}^*(x) \exp(-h_A^*(x)/k_B T) \tag{2}$$

$D_{A0}^*(x)$ is the pre-exponential factor of tracer A diffusion, $h_A^*(x)$ is the enthalpy of diffusion and k_B the Boltzmann constant. The diffusivity of tracer A may then be written in terms of the free enthalpy $g_A^*(x)$,

$$\begin{aligned} g_A^*(x) &= -k_B T \ln [D_A^*(x)/D_{A0}^*(0)] \\ &= h_A^*(x) - s_A^*(x)/k_B \\ h_A^*(x) &= h_{Am}^*(x) + h_{Af}^*(x) \\ s_A^*(x) &= k_B \ln [D_{A0}^*(x)/D_{A0}^*(0)] \end{aligned} \tag{3}$$

$h_A^*(x)$ is the enthalpy, $s_A^*(x)$ the entropy of diffusion of tracer A. The entropy may be obtained by extrapolating tracer diffusivities for different temperatures at constant composition x. The enthalpies of motion $h_{Am}^*(x)$ and of defect formation $h_{Af}^*(x)$ may not be separated without further experiments.

In the analysis of data we have used a second order approximation for $g_A^*(x)$ for each tracer:

$$\begin{aligned} g_A^*(x) &= g_{A0}^* + x\Delta g_{A1}^* + x(1-x)\Delta g_{A2}^* \\ &= h_A^*(0) - x\{k_B T \ln [D_A^*(1)/D_A^*(0)]\} + x(1-x)\Delta g_{A2}^* \end{aligned} \tag{4}$$

The data for tracer diffusion of silver and gold have been fitted (solid lines) according to Eq. (4) by the same fitting parameter $\Delta g_2^* = 0.14$ eV for both tracers Ag and Au with good agreement of data and calculations. Fig. 2 shows tracer diffusion data in Au–Ni alloys at 900°C [10]. The data for tracer diffusion of gold and nickel have again been fitted (solid lines) according to Eq. (4) with good agreement; the upper line is for Au and the lower line is for Ni. The calculated values are $\Delta g_2^* = -0.8$ eV for Au and $\Delta g_2^* = -1.2$ eV for Ni.

If the enthalpy of defect formation is the same for both tracers, we have $h_{Af}^*(x) = h_{Bf}^*(x) = h_f^*(x)$. This will lead to similar values for Δg_2^* for both tracers, as is indeed observed in Ag–Au as well as in Au–Ni. In both alloys the tracers seem to be governed by the same diffusion mechanism.

4. Phase diagram and tracer diffusion in regular solutions

Alloys like Ag–Au and Au–Ni mix in the complete range of composition and we may in most cases expect the same diffusion mechanism for both tracers. Especially for

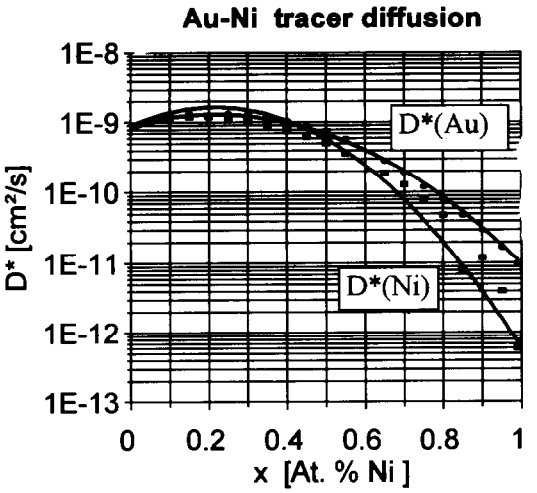

Fig. 2. Tracer diffusion of Au and Ni in Au–Ni alloys as a function of composition x. Data points from Ref. [10], solid line according to Eq. (7).

a vacancy mechanism the concentration of vacancies will be the same for both tracers:

$$n_V(x) = \exp(-h_f^*(x)/k_B T) \tag{5}$$

Metals have, in general, a vacancy concentration close to 10^{-4} at the melting point. This leads to a close relationship between melting temperature T_m and enthalpy of vacancy formation,

$$h_f^*(x) = 4 \ln 10 \times k_B T_m(x) \tag{6}$$

The diffusivities of both tracers will then depend on the melting curve $T(x)$ of the phase diagram. Fig. 3 shows the phase diagram of Ag–Au at the melting point. T_m splits into the solidus and the liquidus line; we may define a mean value of the melting curve, $T_m(x) = 1/2\{T_l + T_s\}$.

Tracer diffusion will then depend on the melting curve $T_m(x)$,

$$\ln D_A^*(x) = \ln D_{A0}^*(x) - h_{Am}^*(x)/k_B T - 4 \ln 10 \times T_m(x)/T\} \tag{7}$$

The negative curvature of $T_m(x)$ of Ag–Au in Fig. 3 contributes to a positive curvature $\Delta g_2^* = 0.14$ eV for both tracer diffusivities $\ln D_{Ag}^*(x)$ and $\ln D_{Au}^*(x)$ in Fig. 1. This indicates that Ag and Au diffuse by a vacancy mechanism in Ag–Au alloys.

On the other hand the positive curvature of $T_m(x)$ of Au–Ni in Fig. 4 contributes to the negative curvatures $\Delta g_2^* = -0.8$ eV for $\ln D_{Au}^*(x)$ and $\Delta g_2^* = -1.2$ eV for $\ln D_{Ni}^*(x)$ in Fig. 2. This indicates that Au and Ni also diffuse by a vacancy mechanism in Au–Ni alloys.

Apparently, in alloys with a vacancy diffusion mechanism the curvature of the mean melting curve $T_m(x)$ generally contributes to the opposite curvature of tracer diffusion for both tracers.

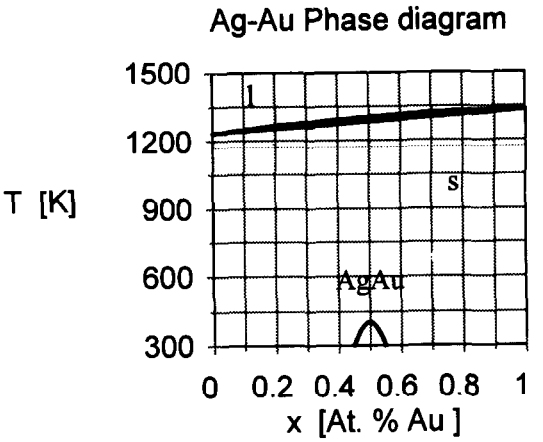

Fig. 3. Phase diagram of Ag–Au; after Ref. [12].

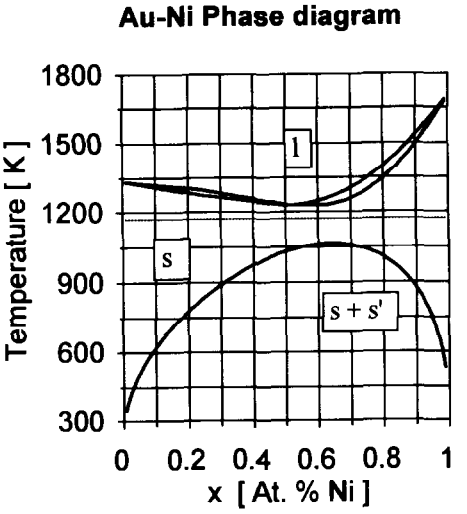

Fig. 4. Phase diagram of Au–Ni; after Ref. [12].

5. Phase diagram and interdiffusion in regular solutions

Interdiffusion—Eq. (1)—depends on the thermodynamic factor $\gamma(x)$. For regular alloys this factor is given by the free enthalpy of mixing [11]

$$\gamma(x) = x(1-x)(\partial^2 g(T, x)/\partial x^2)/k_B T \tag{8}$$

For many binary alloys the model of regular solutions is a good approximation and may be used to calculate the thermodynamic factor $\gamma(x)$ as well as the phase diagram $T(x)$.

The free enthalpy $g(x)$ of mixing in regular binary solids will be

$$g(x) = \varepsilon x[(1-x) - \delta x(1-4x/3)] + k_B T[x \ln x + (1-x)\ln(1-x)] \quad (9)$$

ε is the energy of interaction in binary solids, δ is an asymmetry factor of the phase diagram.

The phase diagram $T_C(x)$ of the binary alloy is calculated from

$$0 = \partial g(T, x)/\partial x \quad (10)$$

$$T_C(x) = \varepsilon(1-2x)(1-2\delta x)/[k_B(\ln(1-x) - \ln x)] \quad (11)$$

$$T_C^{max} = \varepsilon/2k_B \quad (12)$$

In phase diagrams with symmetry in respect of composition, T_C^{max} is the maximum of the critical temperature, above which the tracer atoms will mix at any composition x. Because of asymmetry T_C^{max} may be modified by δ according to Eq. (11) and may only be taken from the fit for the phase diagram.

Fig. 5 shows the phase diagram $T_C(x)$ for Au–Ni alloys for the solid α–α' phases of Fig. 4 in more detail. The data points according to the phase diagram [12] have been fitted with Eq. (6) by the two parameters $T_C^{max} = 813$ K and $\delta = -0.25$.

In Fig. 3 the phase diagram $T_C(x)$ for Ag–Au alloys [12] shows an ordered Ag–Au phase for low temperatures at $x = 0.5$. This indicates an attractive parameter ε or a negative value for T_C^{max}. Because of this symmetry the asymmetry factor is $\delta = 0$.

6. Interdiffusivity $D(x)$

We may now calculate the interdiffusivity of Ag–Au and Au–Ni alloys. According to Eqs. (1)–(12) the coefficient of interdiffusion $D(x)$ will be a function of composition

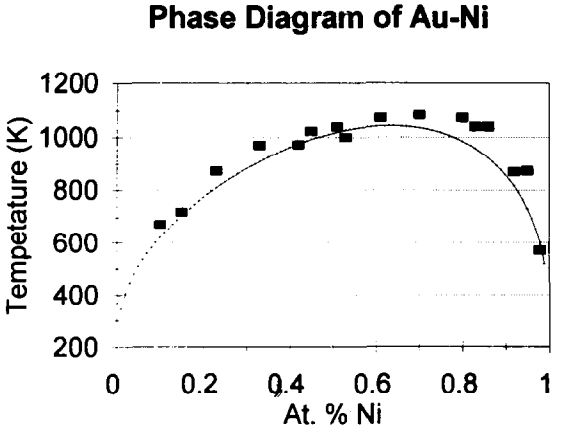

Fig. 5. Solid solid phase diagram of Au–Ni; data from Ref. [12], solid line according to Eq. (11).

x and temperature T:

$$D(x) = \{xD_A^*(x) + (1-x)D_B^*(x)\} \times \{1 - 4[1 + \delta(1-4x)]x(1-x)T_c^{max}/T\} \quad (13)$$

with

$$D_A^*(x) = D_A^*(0)\exp\{x\{k_B T \ln[D_A^*(1)/D_A^*(0)]\} - h_A^*(0) - x(1-x)\Delta g_{A2}^*\}$$

and

$$D_B^*(x) = D_B^*(0)\exp\{x\{k_B T \ln[D_B^*(1)/D_B^*(0)]\} - h_B^*(0) - x(1-x)\Delta g_{B2}^*\}$$

Fig. 6 shows interdiffusion data (squares) in Au–Ni alloys [10] for the annealing temperature $T_1 = 900°C$. Interdiffusivity $D(x)$ calculated according to Eq. (13) is indicated by the solid line. The parameters have been taken from the tracer diffusion data of Fig. 2 and the phase diagram in Fig. 5. The calculations for interdiffusion agree well with the data [10].

In Fig. 6 the curvature of interdiffusion $D(x)$ is mainly negative because of the negative curvature of the tracer diffusivities $D_{Au}^*(x)$ and $D_{Ni}^*(x)$. However, at $x = 0.7$ the interdiffusivity $D(x)$ shows a positive curvature because of the solid α–α' phase transition in Au–Ni. In Fig. 5 the experimental critical temperature at $x = 0.7$ is nearly 1100 K. This is close to the annealing temperature $T_1 = 900°C = 1173$ K. At this point the phase diagram will affect interdiffusion: a positive value of ε or a positive T_C^{max} will contribute to a positive curvature of $D(x)$. Despite the strong negative curvature of the tracer diffusivities $D_{Au}^*(x)$ and $D_{Ni}^*(x)$, in Fig. 6 interdiffusion shows a positive curvature at $x = 0.7$. Interdiffusion will be zero at the spinodale, which is determined by

$$0 = \partial^2 g(T, x)/\partial x^2 \quad (14)$$

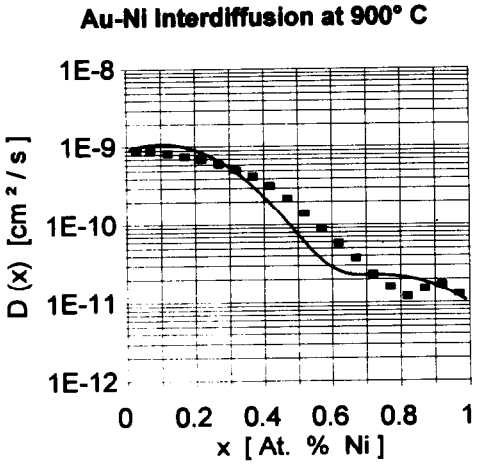

Fig. 6. Interdiffusion of Au–Ni alloys as a function of composition x. Data points from Ref. [10], solid line according to Eq. (13).

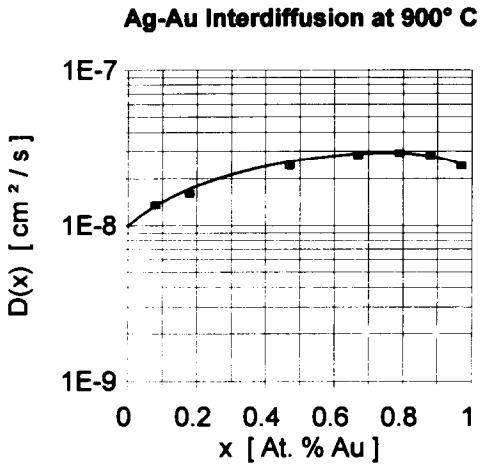

Fig. 7. Interdiffusion of Ag–Au alloys as a function of composition x. Data points from Ref. [9], solid line according to Eq. (13).

Diffusion below the critical temperature $T_C(x)$ will lead to a negative interdiffusivity.

On the other hand, an attractive parameter ε or a negative T_C^{max} will contribute to a negative curvature for interdiffusion $D(x)$, as shown for Ag–Au alloys in Fig. 7. The solid line represents the calculation of interdiffusivity $D(x)$ from tracer diffusivity and the phase diagram according to Eq. (13), and agrees well with the experimental data [9]. The calculations for a negative $T_C^{max} = -400$ K or a negative (attractive) parameter ε lead to negative curvature of interdiffusivity $D(x)$ despite the positive curvature of $D^*_{Ag}(x)$ and $D^*_{Au}(x)$ tracer diffusion in Ag–Au alloys.

7. Conclusions

The agreement of data for tracer diffusion and interdiffusion with phase diagram calculations according to the model of regular alloys is quite satisfying and may lead to further applications in binary and pseudobinary semiconductors.

References

[1] P. Zaumseil, U. Jagdhold and D. Krueger, J. Appl. Phys., 76 (1994) 982–986.
[2] J.-M. Baribeau, J. Appl. Phys., 74 (1994) 3805–3810.
[3] W. Frank, Proc. NATO Advanced Study Inst. on Semiconductor Materials and Processing Technologies, Kluwer Acad. Publishers, Dordrecht, NL, 1992, 383–402.
[4] P.G. Shewmon, Diffusion in Solids, McGraw–Hill, NY, 1960.
[5] B. Tuck, Introduction to Diffusion in Semiconductors, Peregrinus, England, 1974.
[6] R. Fowler and E.A. Guggenheim, Statistical Thermodynamics, Cambridge University Press, 1960.

[7] O.F. Devereux, Topics in Metallurgical Thermodynamics, J. Wiley & Sons, NY, 1963.
[8] L.S. Darken, Trans. AIME, 180 (1949) 430.
[9] W.C. Mallard, A.B. Gardner, R.F. Bass and L.M. Slifkin, Phys. Rev., 129 (1963) 617.
[10] J.E. Reynolds, B.L. Averbach and M. Cohen, Acta Metall., 5 (1957) 29.
[11] J.W. Cahn, Trans. Metall. Soc. AIME, 242 (1968) 166–180.
[12] M. Hansen, Constitution of Binary Alloys, McGraw–Hill, NY, 1958.